Evidence for double acoustic windows in the dolphin, *Tursiops truncatus*

Vladimir V. Popov, Alexander Ya. Supin,[a] Vladimir O. Klishin, Mikhail B. Tarakanov, and Mikhail G. Pletenko
Institute of Ecology and Evolution of the Russian Academy of Sciences, 33 Leninsky Prospect, 119071 Moscow, Russia

(Received 18 June 2007; revised 22 October 2007; accepted 26 October 2007)

In a bottlenose dolphin positions of sound receiving areas on the head surface were determined by comparing the acoustic delays from different sound-source positions. For this investigation, auditory brainstem responses (ABRs) to short tone pips were recorded and their latencies were measured at different sound source positions. After correction for the latency dependence on response amplitude, the difference in ABR latencies was adopted as being the difference of the acoustic delays. These delay differences were used to calculate the position of the sound-receiving point. Measurements were conducted at sound frequencies from 16 to 128 kHz, in half-octave steps. At probe frequencies of 16 and 22.5 kHz, the receiving area was located 21.7–26 cm caudal of the melon tip, which is near the bulla and auditory meatus. At higher probe frequencies, from 32 to 128 kHz, the receiving area was located from 9.3 to 13.1 cm caudal of the melon tip, which corresponds to a proximal part of the lower jaw. Thus, at least two sound-receiving areas (acoustic windows) with different frequency sensitivity were identified. © *2008 Acoustical Society of America.*
[DOI: 10.1121/1.2816564]

PACS number(s): 43.80.Lb [WWA] Pages: 552–560

I. INTRODUCTION

Pathways of sound propagation to the ear of cetaceans, in particular odontocetes (toothed whales, dolphins, and porpoises) are still a matter of discussion (reviewed in detail by Ketten, 1990, 1992a, b, 1997, 2000). As a result of adaptation to underwater hearing conditions, all parts of the odontocete outer, middle, and inner ears are modified as compared to the ear of terrestrial mammals. Therefore, the sound-propagation pathway characteristic of terrestrial mammals (through the external auditory canal and tympanic membrane) does not function in odontocetes. Although some past investigators suggested a role of the external auditory canal for sound transmission in odontocetes (Fraser and Purves, 1954, 1959, 1960), it is currently accepted now that it is not a way of sound propagation to the middle ear. The canal is very narrow, filled with cells and cerumen, and does not connect with the tympanic membrane. Respectively, the tympanic membrane is thick and modified into an elongated, conical structure, the tympanic cone, which does not connect to the middle-ear ossicles. Thus, neither external auditory canal nor tympanic membrane plays the same role in sound reception as in terrestrial mammals.

The best known hypothesis of the sound conduction in cetaceans implicates the lower jaw as the primary pathway (Norris, 1968, 1969, 1980). The dolphin mandibular channel was found to contain a fatty body with an acoustic impedance close to that of sea water (Varanasi and Malins, 1971, 1972). The distal end of the fatty body contacts the outer surface of the lower jaw through a thin bony plate and its proximal end is close to the tympanic bulla which houses the middle ear. It was supposed that sounds enter the fat channel through the thin bony plate, and the channel functions as a specific pathway conducting sounds to the middle ear which is located just near the rear edge of the lower jaw. The region of the lower-jaw surface where sounds enter the fatty body was referred to as the *acoustic window*.

This "mandibular hypothesis" was supported by various data. Both intracranially recorded evoked responses (Bullock *et al.*, 1968) and cochlear action potentials (McCormick *et al.*, 1970, 1980) have revealed the lowest threshold when a sound source is placed on or near the lower jaw. A similar study with the use of a specially designed contact transducer in a suction cup and noninvasively recorded auditory brainstem responses (ABRs) also revealed the highest sensitivity at the middle of the lower jaw surface (Møhl *et al.*, 1999). An attempt to investigate the role of the lower jaw in echolocation performance was made by Brill (1988, 1991) and Brill *et al.* (1988) who placed a sound-shielding neoprene hood on the lower jaw of a dolphin. The hood impaired echolocation performance and this result was considered as evidence in favor of the mandibular hypothesis.

However, not all experimental data could be explained based on the mandibular hypothesis. In evoked-potential experiments, Popov and Supin (1990) determined the location of sound-receiving points by measuring acoustic delays from sound sources of varying positions. In three odontocete species, the sound-receiving point was found to be next to the tympanic bulla and far behind of the lower jaw. On the other hand, those results did not indicate that sounds were transmitted *only* through a point next to the bulla because the delay-vs-azimuth function was more complicated than should be for a single receiving point (Popov *et al.*, 1992).

[a]Author to whom correspondence should be addressed. Electronic mail: alex_supin@mail.ru

Further evidence in favor of multiple sound-receiving points in odontocetes was found when directivity diagrams (threshold-vs-azimuth functions) were measured in a dolphin at various sound frequencies (Popov *et al.*, 2006). The best-sensitivity azimuth depended on sound frequency: the lower the frequency, the more deviation of the best-sensitivity azimuth from the head midline. This feature cannot be explained based on a single receiving aperture since an aperture is always the most sensitive at its axis. Therefore, the data were explained by the presence of two (or more) sound-receiving apertures with different frequency sensitivities: a high-frequency receiving aperture with the axis close to the midline and a low-frequency aperture with the axis deviated from the midline.

Although the presence of more than one acoustic window in cetaceans is seemingly probable, it cannot yet be considered as indisputably confirmed. Little is known concerning the frequency selectivity of the supposed multiple windows. The goal of the present study was to fill in this gap.

To localize acoustic windows, we measured acoustic delays from differently positioned sound sources. The delay measurement was based on latency of the auditory evoked potentials (AEPs). In principle, this method was already used in our preceding studies (Popov and Supin, 1990; Popov *et al.*, 1992). However, the previous studies only used wideband clicks. In the present study, narrowband sound probes were used to investigate how the sound-receiving point position depends on sound frequency.

II. METHODS

A. Measurement paradigm

The principle of the method used to localize sound-receiving points is presented in Fig. 1. Suppose a sound receiving device (the receiver itself or an acoustic window channeled to the receiver) is located in an unknown point X [Fig. 1(a)]. The sound source S is moved around the receiver in a certain manner, for example, by a circle of a radius R with a center at a certain reference point O. The distance d from the sound source to the receiver varies depending on the source angular position: in the presented example, it is the shortest at the position S_1 (distance d_1) and the longest at the position S_2 (distance d_2). If $R \gg r$ (where r is the distance from the reference point O to the receiver X), the distance-vs-angle dependence is a cosine function [Fig. 1(b)] with an amplitude r equal to the distance r from the reference point to the receiver, and the phase shift α equal to the angular position α of the receiver.

The variation of the source-to-receiver distance results in a corresponding variation in the acoustic delay which adds to the latency of responses to the sound signal. The resulting latency variation can be measured experimentally. Assuming that the physiological latency of the response is constant, the variation of the response latency can be attributed to the acoustic delay variation. Conversion of the acoustic delay variation to the distance variation by multiplying by the sound velocity results in a cosine function like that in Fig. 1(b). Its amplitude and phase indicate, respectively, the distance and azimuth of the receiver X relative to the reference point O.

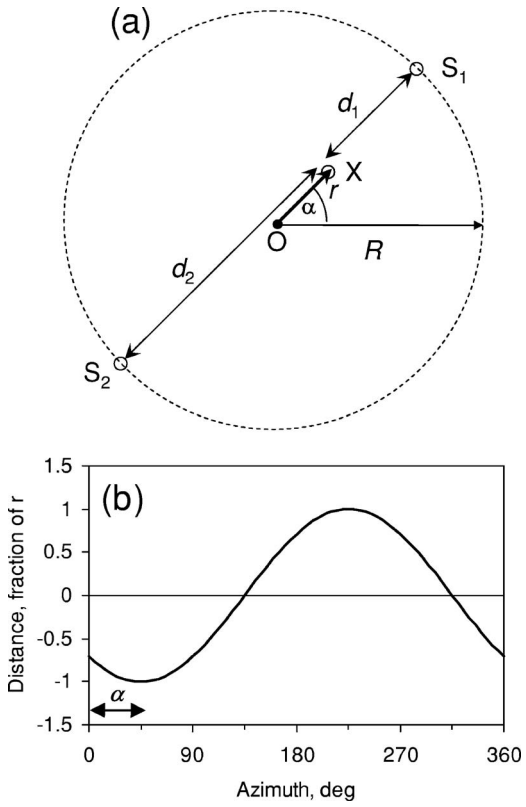

FIG. 1. (a) Experimental paradigm for finding a sound-receiving point by acoustic delays. O—reference point, X—searched-for sound receiving point, S_1 and S_2—opposite positionS of the sound source S, d_1 and d_2—distances from positions S_1 and S_2 to the point X, R—radius of the circle of sound-source movement, r—distance from the reference point O to the point X, α—azimuth of the point X. (b) Dependence of source-to-receiver distance on sound-source azimuth; the middle distance is taken as arbitrary zero; r and α—cosine function amplitude and phase.

If sounds reach a receiver trough a specific channel connecting the receiver and a certain receiving aperture (acoustic window), variation of the acoustic delays reveals the position of the window, because the transmission time through the channel is independent of the sound-source position, and variation of the acoustic delays depends on distance between the sound source and receiving window. Thus, the procedure is appropriate for finding acoustic window positions.

Based on this paradigm, the measurement procedure was adopted as follows:

(i) Auditory evoked responses (AEPs) were recorded to sound stimuli emitted from a number of sound-source positions, all positions at equal distance R from an arbitrarily chosen reference point of the head.

(ii) AEP latencies were measured as a function of the sound-source azimuth.

(iii) Measures were taken to compensate for possible azimuth-dependent variation in the physiological latency.

(iv) The resulting delay-vs-azimuth function was approximated by a cosine function.

(v) The cosine delay-vs-azimuth function was converted to a distance-vs-azimuth function.

(vi) The amplitude and phase of this cosine distance-vs-azimuth function was taken as the distance and azimuth of the receiving point relative to the reference point.

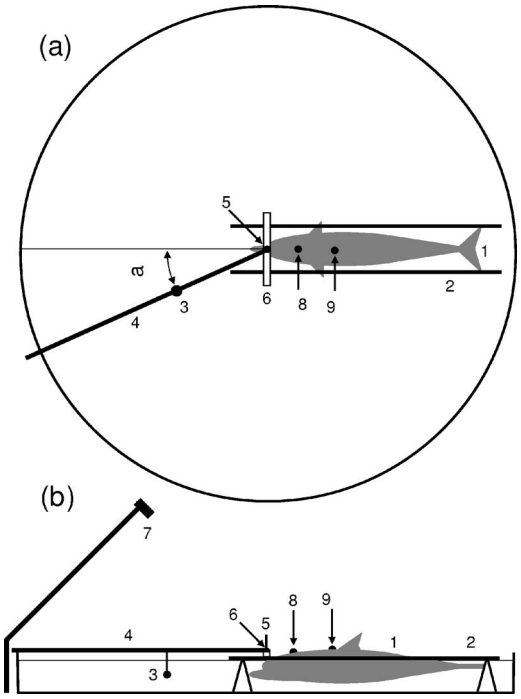

FIG. 2. Experimental design. (a) Dorsal view. (b) Lateral view. Explanation in text.

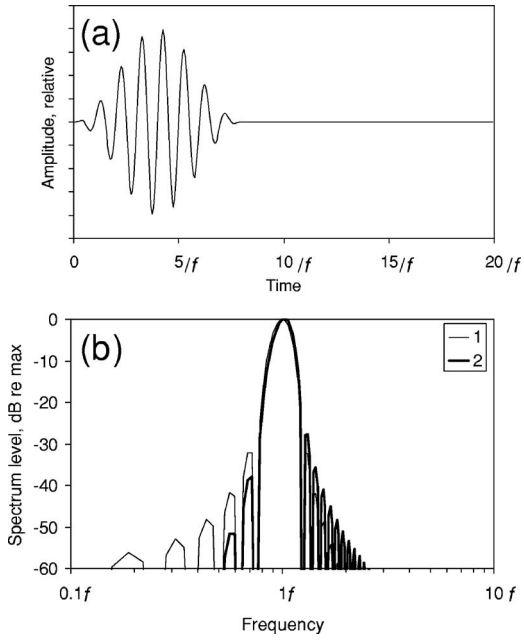

FIG. 3. (a) Stimulus waveform. (b) Stimulus spectrum, 1—electric signal, 2—sound signal played through a transducer frequency response of 12 dB/oct.

B. Subject

The experimental animal was an adult bottlenose dolphin, *Tursiops truncatus*, female, kept in the Utrish Marine Station of the Russian Academy of Sciences on the Black Sea Coast. The animal was housed in an on-land seawater pool $9\times4\times1.2$ m. The use and care of the animal adhered to the guidelines of "Ethical Principles of the Acoustical Society of America for Research Involving Human and Non-Human Animals in Research and Publishing and Presentations."

C. Measurement conditions

During the measurements, the animal was housed in a circular experimental tank filled with sea water, 6 m in diameter, 0.45 m deep (Fig. 2). The animal, (1) rested on a stretcher, (2) was positioned in such a way that the main part of its body was submerged but the blowhole and a part of the back were above water. A sound-emitting transducer (3) was mounted on a bar (4), which could be rotated around a center pin (5) mounted on a support (6). The support (6) was mounted on the stretcher so that the rotation center (5) took one of four positions: above the animal's melon tip, 12.5, 25, or 37.5 cm behind the melon tip, all at the head midline. The animal was positioned in the tank in such a manner that the rotation center coincided with the tank center. The transducer was located at a distance of 1.2 m from the rotation center. Rotation of the bar allowed the placement of the transducer at varying azimuth angles relative to the longitudinal head axis. Since the rotation center coincided with the tank center, the distance from transducer to the tank walls was 1.8 m. Therefore, the path for sounds reflected from the walls to the animal's head was at least 3.6 m longer (the delay at least 2.4 ms longer) than the direct way from the transducer. The position of the animal's head was monitored by a video camera (7).

D. Acoustic stimulation

The acoustic probes were short sound pips [Fig. 3(a)] designed using modulation of a carrier frequency by one cycle of a cosine envelope. Carrier frequencies varied from 16 to 128 kHz by 1/2-octave steps, i.e., 16, 22.5, 32, 45, 64, 90, and 128 kHz. The frequency of the cosine envelope was always 8 times as low as the carrier frequency, that is, from 2 kHz at the 16 kHz carrier to 16 kHz at the 128 kHz carrier. Thus, at all carrier frequencies, the pip contained a constant number (eight) of carrier cycles, and the pip spectrum was constant as expressed on a relative frequency scale [Fig. 3(b,1)]. The primary lobe width of the spectrum was ±0.25 of the carrier frequency, and sidelobes did not exceed −30 dB. Due to deformation of the spectrum by the hydrophone frequency response, the sidelobes were not higher than −37 dB below the main lobe and not higher than −28 dB above the main lobe [Fig. 3(b,2)].

The signals were digitally synthesized and digital-to-analog converted at an update rate of 512 kHz by an acquisition board E-6040 (National Instruments). The analog signals were amplified, attenuated and played through a B&K-8104 transducer. The transducer was placed at a distance of 1.2 m from the rotation center of the transducer-holding bar, at a depth of 22 cm (the mid-depth between the tank bottom and water surface). The stimulus sound pressure levels (peak-to-peak re 1 μPa) were 135 dB at 16 kHz, 140 dB at 22.5 kHz, 145 dB at 32 kHz, 150 dB at 45 kHz, and 160 dB at 64, 90, and 128 kHz. These levels were determined by maximal available voltage of the sound-power amplifier and

frequency response of the transducer. The azimuth position of the transducer varied within a range of ±165° from the longitudinal head axis, in steps of 15°.

E. Evoked-potential recording

Evoked potentials were recorded noninvasively using 1 cm stainless-steel disk electrodes secured at the body surface by rubber suction cups. The active electrode was placed at the vertex midline, 6–7 cm behind the blowhole [Fig. 2(8)]. The reference electrode was placed near the dorsal fin, above the water surface [Fig. 2(9)]. The recorded potentials were amplified, bandpass filtered between 200 and 5000 Hz, digitized at a sampling rate of 40 kHz using a 12 bit analog-to-digital converter and averaged by the data acquisition board E-6040. Each evoked response was collected by averaging 1000 poststimulus sweeps. The program for both stimulus generation and evoked response recording (a "virtual instrument") was designed using LabVIEW software (National Instruments).

F. Computation of the receiving point position

To evaluate the latency difference between AEPs recorded at different sound-source positions, the cross-correlation function (CCF) between these responses was calculated. The lag featuring the highest CCF value was taken as the latency difference.

To compensate for the possible dependence of AEP latency on stimulus efficiency (which may be unequal at different sound-source positions), AEPs were recorded at a constant (zero azimuth) sound-source position and at a variety of stimulus intensities, from the threshold to that producing maximum available (saturation) AEP amplitude. For this series of AEP records, the latency-vs-amplitude dependence was approximated by a straight regression line. The resulting latency-vs-amplitude slope was used to add/subtract a latency correction according to AEP amplitude.

The resulting and corrected latency estimates were averaged between the symmetrical right and left sound-source positions. The resulting latency-vs-azimuth dependence (within an azimuth range from 0° to 165°) was approximated by a 165°-long fragment of a function

$$l(\alpha) = C + d\cos[\pi(\alpha - \varphi)/180],$$

where l (ms) is the latency, C (ms) is a constant, d (ms) is the cosine amplitude, α (degrees) is the azimuth and φ (degrees) is the phase shift. For approximation, the parameters C, d, and φ were iteratively adjusted until reaching the best fit to the experimental data according to the least-mean-square criterion. The resulting value of φ was taken as the direction from the rotation center point to the searched-for sound receiving point and the amplitude d multiplied by the sound velocity was taken as the distance from the rotation center point to the receiving point. The sound velocity was adopted 1505 m/s as calculated by equation of Wilson (1960) at temperature of 22 °C, salinity of 15‰, and pressure of 0.1 MPa. The constant C was ignored as not bearing information of the receiving point position.

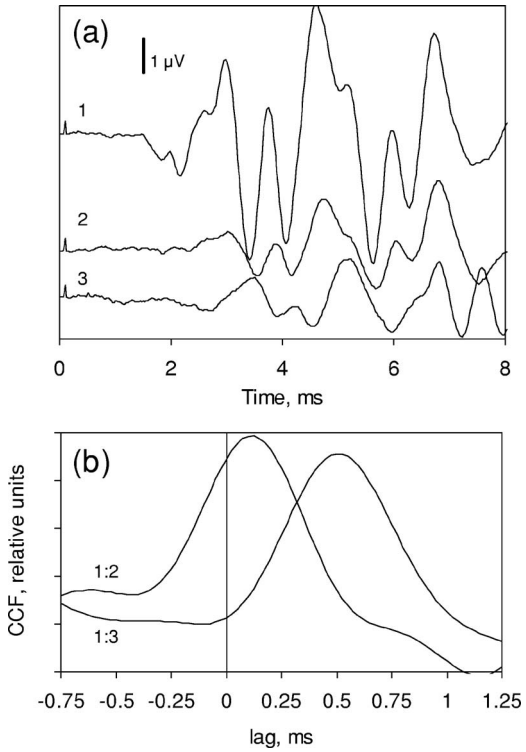

FIG. 4. (a) Examples of ABRs at different sound-source positions and sound intensities. Stimulus frequency 128 kHz. 1—azimuth 0°, intensity 160 dB; 2—0° 125 dB, 3—165° 160 dB. (b) Cross-correlation functions of waveforms 1 and 2 and waveforms 1 and 3 (functions 1:2 and 1:3, respectively).

III. RESULTS

A. AEP waveforms and latencies

Typical AEP waveforms recorded in the present study are exemplified in Fig. 4(a). The responses consisted of a few waves, each shorter than 1 ms, with an overall response duration of 3.5–4 ms and an onset latency of 1.5–2.5 ms. This response waveform was typical of the auditory brainstem evoked responses (ABRs) in odontocete whales, dolphins, and porpoises (rev. Supin *et al.*, 2001).

In many cases, the record contained two similar wave complexes with an interval of 2.4 to 4 ms. This feature is also exemplified in Fig. 4(a). The delay between the two responses corresponds to the delay between sounds directly spreading from the transducer to the animal's head and sound reflected from the nearest tank wall. Therefore, these two wave complexes were considered as responses to direct and reflected sounds, respectively. The delay between the two responses was long enough to measure the amplitude and latency of the first response (to the direct signal) while ignoring the second response (to the reflected sound).

The response latency was dependent on both stimulus intensity and sound-source position. Figure 4(a) exemplifies responses to probes of 128 kHz frequency, from one and the same sound-source position (0° azimuth) but of different intensities: 160 dB (1) and 125 dB re 1 μPa (2). Apart from lower amplitude, the response to lower probe intensity (2) featured longer latency as compared to the response to higher intensity (1). To evaluate the latency difference, a CCF between the waveforms (1) and (2) was calculated [Fig. 4(b)].

This CCF featured its peak at a lag of 0.125 ms; i.e., the waveform (2) was delayed by 0.125 ms relative to the waveform (1).

The influence of sound-source position on the response parameters is also exemplified in Fig. 4. The waveform (3) in Fig. 4(a) presents the response evoked by a sound source of 165° azimuth. The response featured both lower amplitude and longer latency than the response (1) evoked by the probe of 0° azimuth and the same 160 dB intensity. The lower response amplitude indicated lower hearing sensitivity at the 165° azimuth as compared to that at 0°.

The CCF between the waveforms (1) and (3) peaked at a lag of 0.5 ms; i.e., the waveform (3) was delayed by 0.5 ms relative to the waveform (1). This latency difference might be partially attributed to the amplitude-dependent variation. However, there was also a delay between responses (2) and (3) of almost equal amplitudes: the time shift between CCFs (1:2) and (1:3) was 0.375 ms. Assuming that this shift arose because of different acoustic delays, the distances from the two sound source positions to the sound receiver were estimated as differing by 0.375 ms × 150 cm/ms = 56 cm.

B. Acoustic delay dependence on sound-source azimuth

As Fig. 4 shows, AEP latency depended on sound-source azimuth both because of variation of the acoustic delay and because of azimuth-dependent variation of sensitivity which, in turn, influenced the response latency. In the present study, the acoustic delay was the matter of interest. Therefore, for making the necessary compensation possible, it had to be determined, which portion of the azimuth-dependent latency variation was a result of variation of hearing sensitivity.

For this purpose, each measurement session included AEP recordings at a constant (zero) sound source azimuth and at various probe intensities, from response threshold to maximum (saturation), in 5 dB steps. To evaluate both the amplitude variation and the latency shift, CCFs were calculated between the highest of the responses and each of other responses. Figure 5(a) exemplifies the magnitude and latency dependencies on stimulus intensity in a measurement session with a probe frequency of 128 kHz. When the response amplitude reached its maximum ("saturation" at 150 dB), the latency reached its minimum too and did not shorten with further intensity increase up to 160 dB. Thus, the latency variation was associated with the response magnitude rather than with the intensity itself. The latency dependence on response magnitude was nearly a straight line [Fig. 5(b)]. In this particular case, the regression line slope was −0.115 ms/μV.

The next step was AEP recordings at different azimuths, while keeping the probe intensity constant. Using these records, AEP delays relative to that at the zero azimuth were found using the same CCF calculation technique. At each of the sound frequencies, the measurements were repeated four times. The results of the four measurement sets were averaged. Figure 6(a) demonstrates the results of measurements at a probe frequency of 128 kHz and reference point position of 25 cm behind the melon tip, presented as delay-vs-azimuth functions. In this particular measurement session,

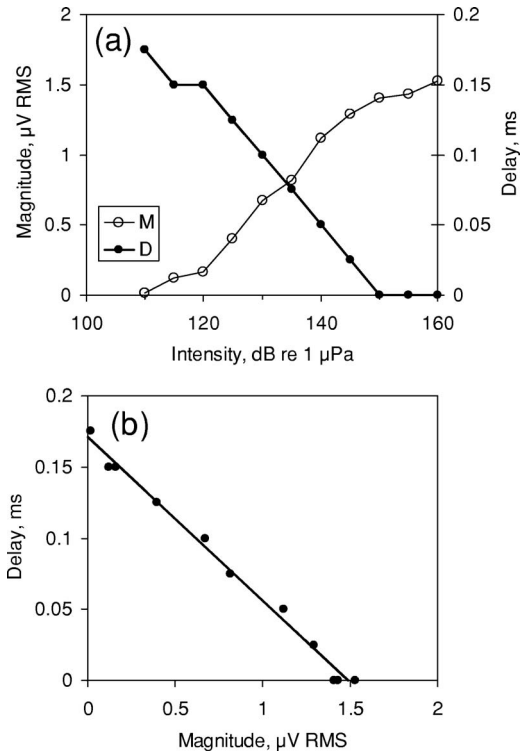

FIG. 5. (a) Dependence of ABR magnitude (M, left scale) and delay relative to the shortest latency (D, right scale) on stimulus intensity. (b) Dependence of ABR delay on magnitude. Stimulus frequency 128 kHz.

both the four original plots and their average featured a minimum latency at the zero azimuth; at all other azimuths, the responses latencies were longer. The delay reached 0.3–0.5 ms at the 165° azimuth.

The response magnitude was also maximal at the zero azimuth [Fig. 6(b)]; thus, a part of the delay-vs-azimuth dependence should be attributed to the latency dependence on response magnitude. Therefore, a correction was done as

$$d_c(\alpha) = d_\alpha + k(m_0 - m_\alpha),$$

where d_c is the corrected delay value at a certain azimuth α, d_α is the original delay value obtained at the azimuth α, m_0 is the response magnitude at the zero (reference) azimuth, m_α is response magnitude at the azimuth α, and k is the delay-vs-magnitude factor. In the measurement session exemplified in Fig. 6, correction using a factor of −0.115 ms/μV (see above, Fig. 5) resulted in a delay-vs-azimuth function presented in Fig. 6(c), 1. This function was adopted as the acoustic delay dependence on azimuth.

Assuming the right and left sound-conductive structures of the head were roughly symmetric, the right and left branches of the found function were symmetrically averaged. Thus, the final delay-vs-azimuth function was obtained by averaging the total of eight measurements within the azimuth range of 0 to 165°. Figure 6(c), 2 presents this average together with standard errors based on both the response delay [Fig. 6(a)] and magnitude [Fig. 6(b)] data scatters. Approximation of this final plot by a 165° fragment of a cosine function gave the best fit to experimental data at a cosine amplitude of 0.14 ms and a phase (minimum delay) of 32°.

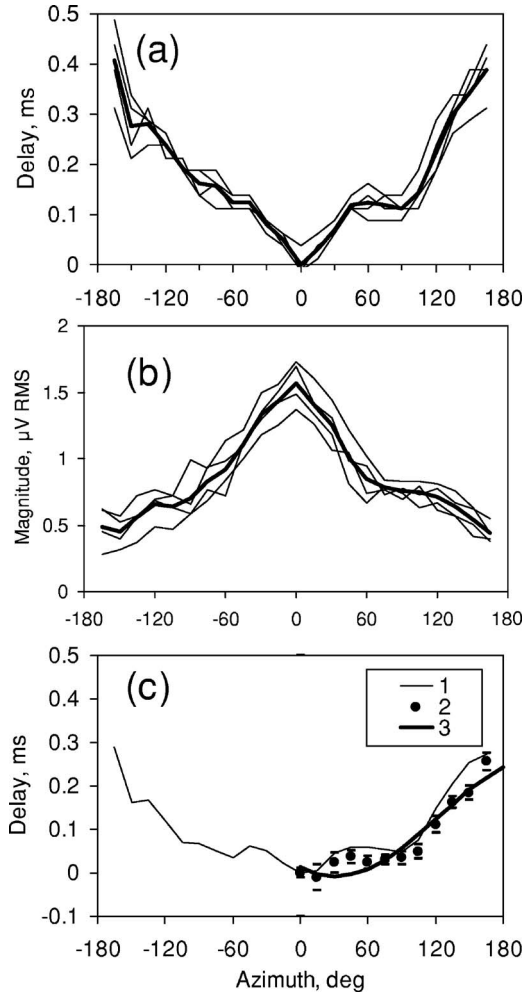

FIG. 6. (a) ABR delay (relative to the shortest latency) dependence on sound-source azimuth. Probe frequency 128 kHz. Thin lines—four sets of measurements, solid line—average of the four. (b) ABR magnitude dependence on sound-source azimuth [thin and solid lines—the same as in (a)]. (c) 1—delay dependence on azimuth corrected for delay-vs-magnitude dependence; 2—average (with standard errors) of the left and right branches of (1); 3—approximating cosine function.

C. Position of sound-receiving points

In the measurement session exemplified above, the obtained parameters of the delay-vs-azimuth function (0.14 ms amplitude, 32° phase) indicated a receiving point at an azimuth of 32° relative to the longitudinal axis and at a distance of $0.14\ \text{ms} \times 150.5\ \text{cm/ms} = 21.1\ \text{cm}$ from the reference point which was 25 cm behind the melon tip. To make the determination of a receiving point more trustworthy, it was repeated in the same manner as described above using four reference (rotation center) points: 0, 12.5, 25, and 37.5 cm behind the melon tip. The results of measurements for a sound frequency of 128 kHz are presented in Fig. 7(a) as four sets of experimental points and approximating cosine functions. Since the shift of a cosine along the ordinate scale does not bear information concerning the receiver position, these functions were arbitrarily shifted to make their zero-azimuth points coincide. Both the amplitudes and phases of the cosine functions were different for different reference points, thus indicating that the found azimuth-dependent delay variation was determined by mutual position of the reference and sound-receiving points.

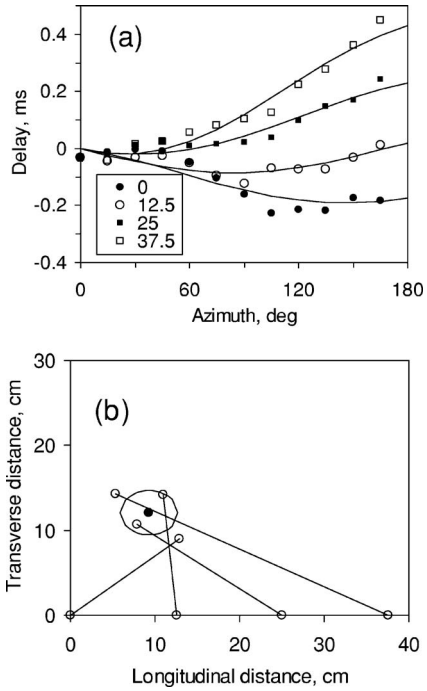

FIG. 7. (a) Determination of a sound receiving point for 128 kHz frequency. (a) Experimental data and approximating cosine function for four reference points, from 0 to 37.5 cm behind the melon tip, as indicated. (b) Vectors drawn from the four reference points according to the cosine function parameters; black solid point—mean of the four found positions; ellipse—SD area.

Parameters (amplitudes and phases) of these four cosine functions were used as lengths and directions of vectors drawn from each of the four reference points [Fig. 7(b)]. Notwithstanding some data scatter, all the vectors indicated a similar area, from 5.3 to 12.9 cm caudal and from 9.0 to 14.3 cm lateral of the melon tip. The mean of these four points was at a point 9.3 cm caudal and 12.1 cm lateral of the melon tip with longitudinal standard deviation (SD) of 3.4 cm and transverse SD of 2.6 cm.

For comparison, results of similar computation for the lowest investigated probe frequency of 16 kHz are presented in Fig. 8. Both the experimental plots and approximating cosine functions presented here obviously differed from those presented above in Fig. 7. Respectively, the vectors drawn according to the cosine parameters indicated another sound-receiving point: the mean of the four points was 21.7 cm caudal and 16.0 cm lateral of the melon tip, with longitudinal SD of 2.3 cm and transverse SD of 11.8 cm; i.e., a point different from that found at 128 kHz probe.

For brevity, we do not present in the same detail all the data obtained at other probe frequencies using the very same procedure. The results of all measurements are presented in Table I as phase (α in degrees) and amplitudes (d in ms) of approximating cosine functions. The results are presented for all the tested probe frequencies (16–128 kHz) and for four positions of the reference points (0–37.5 cm behind the melon tip) for each of the frequencies. Table I presents also the root-mean-square differences between the experimental point arrays and the approximating cosine functions (δd rms, ms). The difference values showed that the approximation

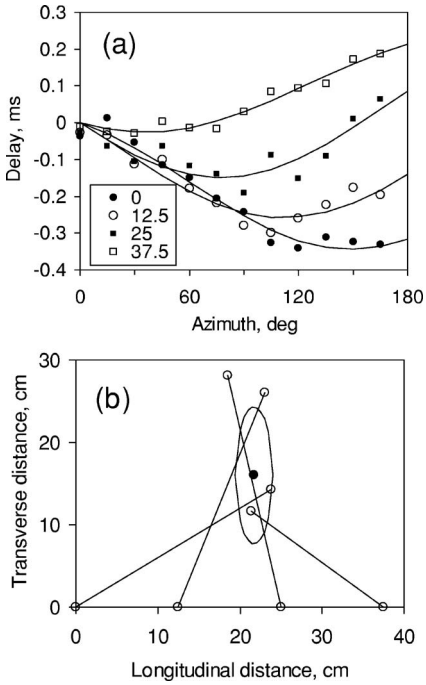

FIG. 8. The same as Fig. 7, for 16 kHz frequency.

was satisfactory enough: in majority of cases (25 of 28 cases, 89%), rms did not exceed 0.04 ms which corresponds to 6 cm distance.

The final result of conversion of the cosine parameters to sound-receiving point positions is presented in Table II and Fig. 9. In Table II, coordinates of receiving points found with the use of four different reference points (0–37.5 cm behind the melon tip) are presented together with SD of the four estimates for each of the probe frequencies (16–128 kHz). In Fig. 9, positions of sound-receiving points are presented together with their SD ellipses superimposed on a diagram of the dorsal view of the dolphin's head. Although the sound-receiving points are shown at the right side of the head, they can be equally attributed to both sides since all the data were obtained by averaging the right- and left-side measurements. The figure shows that all the points dissociated into two groups. Points determined with lower probe frequencies, 16 and 22.5 kHz, were located 21.7–26 cm caudal of the melon tip. The auditory meatus is in this approximate region. Points determined with all higher probe frequencies (32, 45, 64, 90, and 128 kHz) were concentrated in a more rostral area, from 9.3 to 13.1 cm caudal of the melon tip. This is the approximate region of the mandibular acoustic window. SD areas overlapped within each of these two groups but did not overlap between the groups.

IV. DISCUSSION

A. Agreement between the data and measurement paradigm

According to the adopted experimental paradigm, all the delay dependencies on azimuth should fall on cosine functions, and sound-receiver positions obtained at different reference points should coincide. In reality, both the experimental points somewhat deviated from cosine functions and

TABLE I. Parameters of cosine functions approximating experimental data.

F, kHz	Reference point position, cm	Cosine function parameters		
		α,deg	d, ms	δd rms, ms
16	0	149	0.185	0.023
	12.5	112	0.188	0.027
	25	77	0.193	0.035
	37.5	36	0.133	0.014
22.5	0	170	0.175	0.037
	12.5	106	0.088	0.012
	25	92	0.055	0.051
	37	27	0.060	0.040
32	0	157	0.123	0.019
	12.5	97	0.065	0.021
	25	21	0.105	0.018
	37.5	34	0.208	0.030
45	0	148	0.088	0.030
	12.5	88	0.065	0.031
	25	59	0.155	0.033
	37.5	18	0.190	0.026
64	0	144	0.085	0.020
	12.5	100	0.110	0.018
	25	18	0.135	0.047
	37.5	15	0.185	0.017
90	0	158	0.100	0.028
	12.5	95	0.073	0.043
	25	19	0.083	0.028
	37.5	17	0.205	0.037
128	0	145	0.105	0.034
	12.5	84	0.095	0.023
	25	32	0.135	0.026
	37.5	24	0.235	0.031

sound-receiving points obtained at different reference points did not precisely coincide. We suppose that moderate deviations from the theoretical predictions do not contradict the basic measurement paradigm because the method used is very error sensitive. There were at least a few factors which might reduce the precision of measurements.

(i) Background noise might deform AEP records, thus influencing the estimates of their delay. Note that a shift delay estimate by only one record sample (0.025 ms) results in a shift of receiving-point position estimates by 3.75 cm.

(ii) Compensation for response amplitude might not be very precise, both because of spontaneous variation of the response amplitude and because of the difference in latency-vs-amplitude functions at different sound-source azimuths. Note that in some cases, amplitude-dependent variation of delays was as big as around 0.2 ms (see Table I). For example, a compensation error of 10% might result in an error in the delay estimate of 0.02 ms, i.e., which results in an error of 3 cm for the receiving point position.

(iii) Small movements of the animal's head might influence the acoustic delays and therefore the estimates of receiving point positions. The range of the error might be of the same order of magnitude as the range of head movements, up to a few cm.

Taking into consideration all these factors, significant data scatter seemed inevitable. Bearing this in mind, each receiving point position was computed based on 48 delays

TABLE II. Estimates of receiving point positions.

F, kHz	Reference point position, cm	Receiving point coordinates					
		X, cm	Y, cm	Average X, cm	Average Y, cm	SD(X), cm	SD(Y), cm
16	0	23.8	14.3				
	12.5	23.0	26.1	21.7	16.0	2.3	8.3
	25	18.5	28.1				
	37.5	21.4	11.7				
22.5	0	32.9	5.8				
	12.5	16.1	12.6	26.0	6.1	7.2	3.7
	25	25.7	8.2				
	37.5	29.5	4.1				
32	0	16.9	7.2				
	12.5	13.7	9.7	13.1	8.0	2.9	5.3
	25	10.3	5.6				
	37.5	11.7	17.4				
45	0	11.1	7.0				
	12.5	12.2	9.7	11.7	9.1	1.2	5.7
	25	13.0	19.9				
	37.5	10.4	8.8				
64	0	10.3	7.5				
	12.5	15.4	16.2	10.5	7.4	3.9	4.7
	25	5.7	6.3				
	37.5	10.7	7.2				
90	0	13.9	5.6				
	12.5	13.5	10.8	12.2	5.9	2.7	8.3
	25	13.3	4.0				
	37.5	8.1	9.0				
128	0	12.9	9.0				
	12.5	11.0	14.2	9.3	12.1	3.4	2.6
	25	7.8	10.7				
	37.5	5.3	14.3				

X and Y—coordinates along the longitudinal (X) and transverse (Y) head axes, adopting the melon tip as zero; SD(X) and SD(Y)—standard deviations among four estimates of X and Y coordinates, respectively.

(12 sound-source azimuths at each of four reference points), although theoretically three delays are necessary to compute a receiver position. The deviations of experimental data from a cosine function did not exceed a few cm rms (see Table I); i.e., of the same order as may be expected due to the reasons considered above. The differences in receiving-point positions computed at different reference points did not exceed a few cm either for one and the same probe frequency (see Table II). Therefore, the obtained deviation of experimental data from true cosine functions does not contradict the basic paradigm.

B. Validity of the unilateral model

Computations described above imply that the sound is perceived by an acoustical window (windows) at only one side, ipsilateral to the sound source position. Basing on this assumption, results of left- and right-side measurements were averaged. Validity of this approach needs a comment. As shown before (Popov *et al.*, 2006), at all sound frequencies from 16 to 128 kHz, interaural intensity difference in the bottlenose dolphin reaches from 10 to 30 dB at azimuths above 15°. As Fig. 5 shows, this intensity difference resulted in big difference of AEP amplitude. Therefore, we expected that contribution of the contralateral input, if existed, little influenced temporal parameters of AEP. Assuming this suggestion, the unilateral model may be taken as valid.

C. Multiple receiving areas

The main result of the investigation presented here is the presence of at least two sound-receiving areas on the dolphin head: a rostral (9–12 cm behind the melon tip) and a caudal (21–26 cm behind the melon tip) area. The rostral sound receiving area manifested itself at probe frequencies of 32 kHz and higher, the caudal at probe frequencies of 22.5 kHz and lower. Within each of these two areas, there is no frequency-dependent regularity of receiving point positions, and SD areas of all points overlap; on the contrary, there is no SD overlap between the two areas. Thus, there is no continuous frequency-dependent shift of the sound-receiving point position but there are two separate sound-receiving areas.

The rostral sound-receiving area coincides well with the position of the mandibular acoustic window hypothesized before. Thus, the results of the present study confirm once again this hypothesis. As to the caudal sound-receiving area, its presence confirms the hypothesis of possibility of sound transmission through a near-bullar area (Popov and Supin, 1990; Popov *et al.*, 1992).

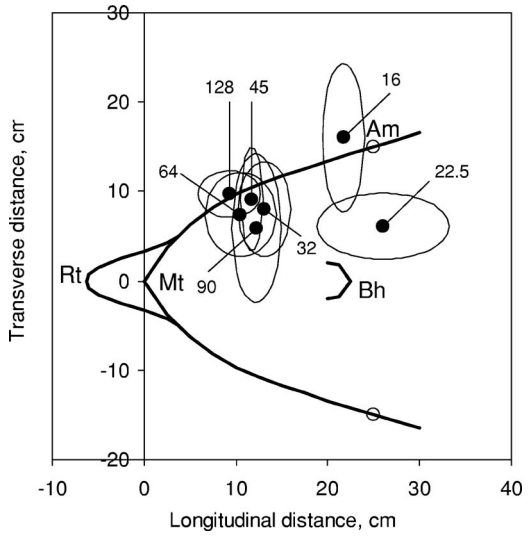

FIG. 9. Positions of sound-receiving points for frequencies from 16 to 128 kHz. Each position (solid dot) is an average of four positions found with four different reference points. Ellipses delimit SD areas for each sound-receiving point. Point positions are superimposed on a contour of the dorsal view of the dolphin's head. Rt—rostrum tip, Mt—melon tip, Bh—blowhole, Am—auditory meatus.

The results presented herein show that there is no contradiction between these two hypotheses. The two sound-receiving areas (acoustic windows) have different frequency sensitivities. In all studies of acoustic window localization performed before, wideband acoustic probes were used. So depending on stimulus parameters and experimental design, either of these two areas could be detected. A hypothesis of more than one sound-receiving area has also a morphological confirmation: a few sound-conduction pathways may be provided by a few lobes of fatty tissues connecting to the bulla (Ketten, 2000).

The significance of multiple sound-receiving areas is not clear yet. However, some speculative hypotheses can be suggested. Because of different frequency sensitivity of sound-receiving areas, the best-sensitivity axis direction may be frequency dependent (Popov *et al.*, 2006). A result of such dependence is that a perceived spectral pattern of a broadband sound stimulus depends, in turn, on the sound direction. It may provide additional cues for both localization of sound sources and sound pattern recognition.

ACKNOWLEDGMENTS

The study was supported by The Russian Ministry of Science and Education, Grant No. NSh-7117.2006.4 and The Russian Foundation for Basic Research, Grant No. 06-04-48518. The authors thank the staff of the Utrish Marine Station (supervised by Lev Mukhametov) for assistance.

Brill, R. L. (**1988**). "The jaw-hearing dolphin: Preliminary behavioral and acoustical evidence," in *Animal Sonar: Processes and Performance*, edited by P. E. Nachtigall and P. W. B. Moore (Plenum, New York), pp. 281–287.

Brill, R. L. (**1991**). "The effect of attenuating returning echolocation signals at the lower jaw of a dolphin (*Tursiops truncatus*)," J. Acoust. Soc. Am. **89**, 2851–2857.

Brill, R. L., Sevenich, M. L., Sullivan, T. J., Sustman, J. D., and Witt, R. E. (**1988**). "Behavioral evidence for hearing through the lower jaw by an echolocating dolphin, *Tursiops truncatus*," Marine Mammal Sci. **4**, 223–230.

Bullock, T. H., Grinnell, A. D., Ikezono, F., Kameda, K., Katsuki, Y., Nomoto, M., Sato, O., Suga, N., and Yanagisava, K. (**1968**). "Electrophysiological studies of the central auditory mechanisms in cetaceans," Z. Vergl. Physiol. **59**, 117–156.

Fraser, F. C., and Purves, P. E. (**1954**). "Hearing in cetaceans," Bull. British Mus. (Nat. Hist.) **2**, 103–116.

Fraser, F. C., and Purves, P. E. (**1959**). "Hearing in whales," Endeavour **18**, 93–98.

Fraser, F. C., and Purves, P. E. (**1960**). "Hearing in cetaceans: Evolution of the accessory air sacs and the structure and function of the outer and middle ear in recent cetaceans," Bull. British Mus. (Nat. Hist.) **7**, 1–140.

Ketten, D. R. (**1990**). "Three-dimensional reconstructions of the dolphin ear," in *Sensory Abilities of Cetaceans. Laboratory and Field Evidence*, edited by J. A. Thomas and R. A. Kastelein (Plenum, New York), pp. 81–105.

Ketten, D. R. (**1992a**). "The cetacean ear: Form, frequency, and evolution," in *Marine Mammal Sensory Systems*, edited by J. A. Thomas, R. A. Kastelein, and A. Ya. Supin (Plenum, New York), pp. 53–75.

Ketten, D. R. (**1992b**). "The marine mammal ear: Specialization for aquatic audition and echolocation," in *The Evolutionary Biology of Hearing*, edited by D. Webster, R. R. Fay, and A. N. Popper (Springer, New York), pp. 717–754.

Ketten, D. R. (**1997**). "Structure and function in whale ears," Bioacoustics **8**, 103–135.

Ketten, D. R. (**2000**). "Cetacean ears," in *Hearing by Whales and Dolphins*, edited by W. W. L. Au, A. N. Popper, and R. R. Fay (Springer, New York), pp. 43–108.

McCormick, J. G., Wever, E. G., Palin, G., and Ridgway, S. H. (**1970**). "Sound conduction in the dolphin ear," J. Acoust. Soc. Am. **48**, 1418–1428.

McCormick, J. G., Wever, E. G., Ridgway, S. H., and Palin, G. (**1980**). "Sound reception in the porpoise as it relates to echolocation," in *Animal Sonar Systems*, edited by R. G. Busnel and J. F. Fish (Plenum, New York), pp. 449–467.

Møhl, B., Au, W. W. L., Pawloski, J., and Nachtigall, P. E. (**1999**). "Dolphin hearing: Relative sensitivity as a function of point of application of a contact sound source in the jaw and head region," J. Acoust. Soc. Am. **105**, 3421–3424.

Norris, K. S. (**1968**). "The evolution of acoustic mechanisms in odontocete cetaceans," in *Evolution and Environment*, edited by E. T. Drake (Yale University, New Haven), pp. 297–324.

Norris, K. S. (**1969**). "The echolocation of marine mammals," in *The Biology of Marine Mammals*, edited by H. J. Andersen (Academic, New York), pp. 391–424.

Norris, K. S. (**1980**). "Peripheral sound processing in odontocetes," in *Animal Sonar System*, edited by R.-G. Busnel and J. F. Fish (Plenum, New York), pp. 495–509.

Popov, V. V., and Supin, A. Ya. (**1990**). "Localization of the acoustic window at the dolphin's head," in: *Sensory Abilities of Cetaceans: Laboratory and Field Evidence*, edited by J. A. Thomas and R. A. Kastelein (Plenum, New York), pp. 417–426.

Popov, V. V., Supin, A. Ya., and Klishin, V. O. (**1992**). "Electrophysiological study of sound conduction in dolphins," in *Marine Mammal Sensory Systems*, edited by J. A. Thomas, R. A. Kastelein, and A. Ya. Supin (Plenum, New York), pp. 269–276.

Popov, V. V., Supin, A. Ya., Klishin, V. O., and Bulgakova, T. N. (**2006**). "Monaural and binaural hearing directivity in the bottlenose dolphin: Evoked-potential study," J. Acoust. Soc. Am. **119**, 636–644.

Supin, A. Y., Popov, V. V., and Mass, A. M. (**2001**). *The Sensory Physiology of Aquatic Mammals* (Kluwer, Boston), 332 pages.

Varanasi, U., and Malins, D. C. (**1971**). "Unique lipids of the porpoise (*Tursiops gilli*): Difference in triacylglycerols and wax esters of acoustic (mandibular and melon) and blubber tissues," Biochim. Biophys. Acta **23**, 415–418.

Varanasi, U., and Malins, D. C. (**1972**). "Triacylglycerols characteristics of porpoise acoustic tissues: Molecular structures of diisovaleroylglycerides," Science **176**, 926–928.

Wilson, W. D. (**1960**). "Equation for the speed of sound in sea water," J. Acoust. Soc. Am. **32**, 1357.